Draft version February 5, 2008
Preprint typeset using LaTeX style emulateapj v. 6/22/04

THE INFLUENCE OF BARYONS ON THE CLUSTERING OF MATTER AND WEAK LENSING SURVEYS

Y. P. Jing[1,4], Pengjie Zhang[1,4], W.P. Lin[1,4], L. Gao[2,3], V. Springel[2]
[1] Shanghai Astronomical Observatory, Nandan Road 80, Shanghai, China
[2] Max-Planck-Institut für Astrophysik, Karl-Schwarzschild-Strasse 1, 85748 Garching, Germany
[3] Institute for Computational Cosmology, Physics Department, Durham. U.K.
[4] Joint Institute for Galaxy and Cosmology (JOINGC) of SHAO and USTC and
e-mail: ypjing@shao.ac.cn

Draft version February 5, 2008

ABSTRACT

Future weak lensing measurements of cosmic shear will reach such high accuracy that second order effects in weak lensing modeling, like the influence of baryons on structure formation, become important. We use a controlled set of high-resolution cosmological simulations to quantify this effect by comparing pure N-body dark matter runs with corresponding hydrodynamical simulations, carried out both in non-radiative, and in dissipative form with cooling and star formation. In both hydrodynamical simulations, the clustering of the gas is suppressed while that of dark matter is boosted at scales $k > 1\,h\mathrm{Mpc}^{-1}$. Despite this counterbalance between dark matter and gas, the clustering of the total matter is suppressed by up to 1 percent at $1 \lesssim k \lesssim 10\,h\mathrm{Mpc}^{-1}$, while for $k \approx 20\,h\mathrm{Mpc}^{-1}$ it is boosted, up to 2 percent in the non-radiative run and 10 percent in the run with star formation. The stellar mass formed in the latter is highly biased relative to the dark matter in the pure N-body simulation. Using our power spectrum measurements to predict the effect of baryons on the weak lensing signal at $100 < l < 10000$, we find that baryons may change the lensing power spectrum by less than 0.5 percent at $l < 1000$, but by 1 to 10 percent at $1000 < l < 10000$. The size of the effect exceeds the predicted accuracy of future lensing power spectrum measurements and will likely be detected. Precise determinations of cosmological parameters with weak lensing, and studies of small-scale fluctuations and clustering, therefore rely on properly including baryonic physics.

Subject headings: gravitational lensing—dark matter— cosmology: theory— galaxies: formation

1. INTRODUCTION

Weak gravitational lensing directly measures the projected mass distribution and is emerging as one of the most powerful and robust probes of the large scale structure of the universe, and the nature of dark matter, dark energy and gravity (Huterer 2002; Hu 2002; Jain & Taylor 2003; Takada & Jain 2004; Ishak et al. 2005; Knox et al. 2005). Ongoing and upcoming surveys such as CFHTLS[1], DES[2], LSST[3], Pan-STARRS[4], SKA[5] and SNAP[6] will significantly reduce statistical errors in lensing power spectrum measurements to the $< 1\%$ level at $l \sim 1000$. As new analysis techniques enable a significant reduction of systematic errors in cosmic shear (Jarvis & Jain 2004; Jain et al. 2005; Heymans et al. 2005, and references therein) and cosmic magnification measurements (Ménard & Bartelmann 2002; Scranton et al. 2005; Zhang & Pen 2005a,b), weak lensing measurement is quickly entering the precision era. To match this accuracy, many simplifications in theoretical modeling have to be scrutinized in detail (Bernardeau 1998; Schneider et al. 1998; Dodelson & Zhang 2005; Dodelson et al. 2005; White 2005).

A widely adopted simplification in weak lensing modeling is the assumption that baryons trace dark matter perfectly. With this simplification, weak lensing involves only gravity and collision-less dark matter dynamics, allowing it to be accurately predicted with the aid of N-body simulations. However, on small scales, baryons *do not follow* the dark matter distribution. Recently, White (2004) and Zhan & Knox (2004) estimated the effects of cooling gas and intra-cluster gas on the lensing power spectrum, respectively. These two components of baryons can both have an effect of a few percent on the lensing power spectrum at $l \sim 3000$, but with opposite signs. Such effects exceed future measurement errors and are certainly relevant in order to exploit the full power of precision measurements of weak lensing. However, analytical models are simplified with *ad hoc* parameters and lack the ability to deal with back-reactions of baryons on the dark matter. They can not robustly answer several key questions such as (1) to what level the two effects cancel, (2) at what scales each of them dominates, and (3) how large the effect is for the non-virialized intergalactic medium where most of the baryons reside. To quantify the effect of baryons on lensing statistics accurately, it is hence necessary to use hydrodynamical simulations with all relevant gas physics included. In this *letter*, we analyze a controlled set of simulations to address this issue.

2. BARYONIC EFFECT ON THE CLUSTERING OF COSMIC MATTER

2.1. *Simulations*

We use the GADGET2 code (Springel et al. 2001; Springel 2005) to simulate structure formation in a concordance cosmological model. The cosmological and initial density fluctuation parameters of the model are

[1] http://www.cfht.hawaii.edu/Science/CFHLS
[2] http://www.darkenergysurvey.org/
[3] http://www.lsst.org/
[4] http://pan-starrs.ifa.hawaii.edu/
[5] http://www.skatelescope.org/
[6] http://snap.lbl.gov/

$(\Omega_m, \Omega_\Lambda, \Omega_b, \sigma_8, n, h)$=$(0.268, 0.732, 0.044, 0.85, 1, 0.71)$. Three simulations were run with the same initial fluctuations for a cubic box of 100 h^{-1}Mpc. The first simulation is a pure dark matter cosmological simulation. The second one is a gas simulation where no radiative cooling of gas is considered. The last run is a gas simulation that includes the physical processes of radiative cooling and star formation. It also includes supernova feedback, outflows by galactic winds, and a sub-resolution multiphase model for the interstellar medium as detailed in Springel & Hernquist (2003). In all simulations, we use 512^3 particles to represent each component of dark matter and gas.

Uncertainties in simulating star formation could bias our study. To check the robustness of our star formation run, we measured the stellar mass density $\Omega_\star$ in units of the critical density at $z = 0$. We found $\Omega_\star = 0.0034$. This is in reasonable agreement with recent observational results (e.g. Fukugita et al. (1998, $\Omega_\star = 0.0035$), Bell et al. (2003, $\Omega_\star = 0.0028 \pm 0.0008$)). The star formation history of the simulation is therefore close enough to reality for the purposes of the present paper.

2.2. *Clustering in the non-radiative run*

We measure the mass power spectrum $P(k)$ for matter, gas and stars separately, as well as for the total matter density in the simulations. The Triangular Shaped Cloud (TSC) interpolation function $W(r)$ is used to obtain the smoothed density field on a uniform grid of 1024^3 cells, and the power spectrum is determined from the Fourier transform of the density field. We use the method of Jing (2005) to correct for the smoothing and aliasing effects caused by the TSC mass interpolation and for the noise caused by the particle discreteness.

The power spectrum of each matter component is plotted in Figure 1 for redshifts $z = 0$ and $z = 1$. Here we use the mass variance $\Delta^2(k)$ per logarithmic interval in wavelength which is related to $P(k)$ by $\Delta^2(k) = 4\pi k^3 P(k)/(2\pi)^3$. According to the extensive tests of Hou et al. (2005), the power spectrum is affected by the force resolution at $k > k_\eta \approx 0.3 \times 2\pi/\eta$, where η is the Plummer-equivalent force softening length used in the simulation. In our simulations, $\eta = 5\,h^{-1}$kpc for the pure dark matter and non-radiative runs, and $\eta = 9\,h^{-1}$kpc for the star formation run. Down to the scale of $k \approx 20\,h$Mpc^{-1}, the force resolution should have negligible effects.

Comparing the results of the pure dark matter and the non-radiative runs, one finds that the gas has a weaker clustering than the dark matter on small scales ($k > 1\,h$Mpc^{-1}). This can be interpreted as the result of gas pressure which reduces small-scale structure in the gas distribution. Zhan & Knox (2004) approximated the hot baryon distribution by assuming that the gas is in hydrostatic equilibrium in NFW dark halos (Makino et al. 1998), and found a qualitatively similar result. But quantitatively, the gas clustering suppression in their simple analytic estimate is stronger than our simulations indicate. At $k = 10\,h$Mpc^{-1} and $z = 0$, the $\Delta^2(k)$ of gas is 25 percent lower than that of dark matter in our non-radiative simulation (see Figure 2), while the $\Delta^2(k)$ of gas is 50 percent lower in their analytic estimate. We also see a more extended baryonic effect at $k < 1\,h$Mpc^{-1}

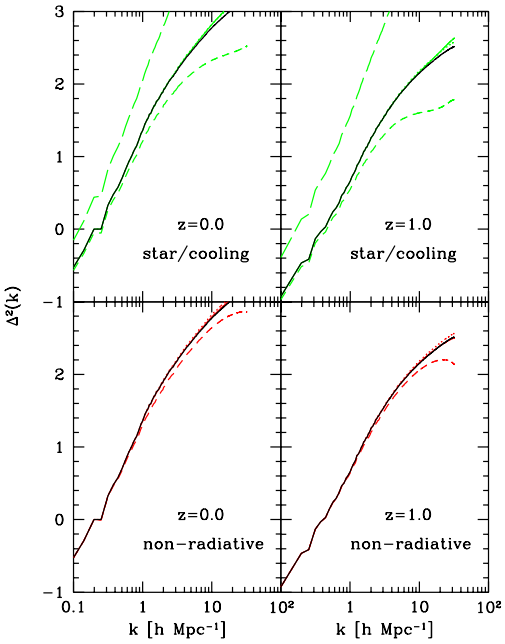

FIG. 1.— The power spectrum of density fluctuations of each matter component in the non-radiative gas simulation (bottom panels), and in the gas cooling and star formation simulation (top panels), at redshifts $z = 1$ and $z = 0$. The results are compared with the spectrum of the pure dark matter simulation (black solid lines). The colored dotted lines, dashed lines, long dashed lines, and solid lines are plotted for the dark matter, gas, stellar and total matter density field, respectively.

which may be caused by filaments and is beyond the exploration of their halo model. These effects indicate the need for hydrodynamical simulations to accurately assess the effect of baryons on the clustering of cosmic matter.

An interesting result from our non-radiative simulation is that its dark matter has a stronger clustering than found in the pure dark matter run. To show the difference clearly, we plot it separately in Figure 2, where we also show the clustering differences of other matter components relative to the pure dark matter run. The dark matter clustering is a few percent stronger in the non-radiative cooling simulation at $k > 1\,h$Mpc^{-1}, and is more than 10% stronger at $k > 10\,h$Mpc^{-1}. This behavior can be understood as a result of the gravitational back reaction due to hot gas, since the gas is hotter than the dark matter virial temperature in the central regions of dark halos, due to its collisional nature (see, Rasia et al. 2004; Lin et al. 2006).

Compared to the power spectra of gas and dark matter, the $P_{\rm NR}^{\rm tot}(k)$ of the total matter distribution in the non-radiative run differs less dramatically from the $P_{\rm DM}(k)$ of the pure dark matter run[7], because the baryonic suppression of the gas clustering is partially counterbalanced by its effect on the dark matter. However, there still exists a significant difference in the total matter clustering between the two runs (see Figures 1 and 2). The total matter spectrum $P_{\rm NR}^{\rm tot}(k)$ is a few percent lower

[7] Here we use the subscripts DM, NR, SF for the pure dark matter, non-radiative, and star formation runs, respectively, and the superscripts dm, gas, star, and tot for each matter component.

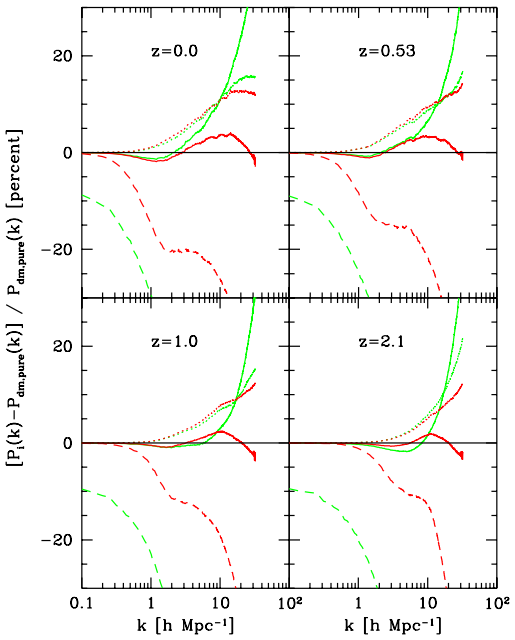

FIG. 2.— The influence of baryons on the clustering of each matter component. The plot shows the relative difference (in percent) of the power spectrum of each matter component in the gas simulations relative to the pure dark matter simulation. The results of the non-radiative run are plotted with red color, and those of the star formation run with green colors. The colored dotted lines, dashed lines, and solid lines are plotted for the dark matter and gaseous components, and the total matter density field, respectively. The stellar component in the star formation run is omitted here, as the difference can be easily infered from Figure 1.

than $P_{\rm DM}(k)$ at $k \approx 2\,h{\rm Mpc}^{-1}$, and is a few percent higher than $P_{\rm DM}(k)$ at $k \approx 10\,h{\rm Mpc}^{-1}$. At the smaller scales, the difference becomes smaller because $P_{\rm NR}^{\rm gas}(k)$ drops faster than $P_{\rm NR}^{\rm dm}(k)$ increases. Although the formal gravitational resolution limit of the simulation is $k \approx 40\,h{\rm Mpc}^{-1}$, hydrodynamical convergence can only be expected on somewhat larger scales, thus it will be interesting to check the results at $k > 10\,h{\rm Mpc}^{-1}$ shown in Figure 2 with higher resolution simulations.

2.3. *Clustering in the simulation with star formation*

In our star formation run, the stellar matter is found to be significantly more clustered than dark matter or gas (Figure 1). Its power spectrum $P_{\rm SF}^{\rm star}(k)$ is a few times higher than the dark matter counterpart $P_{\rm SF}^{\rm dm}(k)$, and the bias factor increases towards smaller scales. This result is expected, because the stars can form only in high density regions and thus are highly biased tracers of the matter distribution.

On the other hand, the power spectrum of gas $P_{\rm SF}^{\rm gas}(k)$ is significantly lower than $P_{\rm SF}^{\rm dm}(k)$. Apart from the mild effects of shock heating and gas pressure that can be infered from the non-radiative simulation, the main reason is that gas is under-represented relative to the dark matter in high density regions, where part of the gas has cooled and turned into stars. Because of this anti-bias, $P_{\rm SF}^{\rm gas}(k)$ is always smaller by $\sim 10\%$ than $P_{\rm SF}^{\rm dm}(k)$ even on large scales (Figure 2), and drops much faster at small scales than the counterpart $P_{\rm NR}^{\rm gas}(k)$ in the non-radiative run. The power spectrum of dark matter $P_{\rm SF}^{\rm dm}(k)$ looks very similar to the counterpart $P_{\rm NR}^{\rm dm}(k)$ in the non-radiative run, except the former is higher at $k > 10\,h{\rm Mpc}^{-1}$ because of the baryon condensation in the star formation run.

The power spectrum of the total matter density $P_{\rm SF}^{\rm tot}(k)$ shows a similar decrease at $k \lesssim 2\,h{\rm Mpc}^{-1}$ as found in the non-radiative run. As we discussed before, this behavior is mainly due to shock heating and the thermal pressure of the gas. This is confirmed in our star formation run, indicating that this feature is robust against the star formation processes. The $P_{\rm SF}^{\rm tot}(k)$ is higher than $P_{\rm NR}^{\rm tot}(k)$ at $k > 10\,h{\rm Mpc}^{-1}$ at $z < 1$, which is mainly caused by the baryon condensation due to gas cooling. We also note that $P_{\rm SF}^{\rm tot}(k)$ is slightly lower at $k \approx 8\,h{\rm Mpc}^{-1}$ than the counterparts $P_{\rm NR}^{\rm tot}(k)$ and $P_{\rm DM}(k)$ at $z \gtrsim 1$, which likely results from the feedback heating due to active star formation at high redshift.

3. THE BARYONIC EFFECT ON WEAK LENSING

In this section, we study the influence of baryons on the weak lensing shear power spectrum C_l. We use Limber's approximation (Limber 1954) to calculate C_l from the simulated $P^{\rm tot}$. For a flat universe, C_l and $P^{\rm tot}$ are related by

$$C_l = \left(\frac{3\Omega_m H_0^2}{2c^2}\right)^2 \int P^{\rm tot}\left(\frac{l}{\chi}, z\right) W^2(\chi,\chi_s)\chi^{-2}{\rm d}\chi \ , \quad (1)$$

where $W(\chi,\chi_s) = (1+z)\chi(1-\chi/\chi_s)$ is the lensing kernel, and χ_s and χ are the comoving angular diameter distances to the source and lens, respectively.

In Figure 3, we show the effect of the baryons on the weak lensing power spectrum by assuming that the lensed sources are at redshifts $z_s = 0.6$, 1.0, and 1.5, respectively. For the non-radiative run, the lensing power signal is suppressed by less than one percent at $100 < l < 1000$ and is then enhanced to about 1% at $l = 4000$. The detailed behavior depends on the source redshift, and the relative change of C_l increases with the decrease of z_s. This is expected since the baryons have more significant effects at lower redshifts (Figure 2).

Including more realistic star formation processes compensates for the lensing power suppression at $100 < l < 1000$ seen in the non-radiative run. As a result, the change of the lensing power by the presence of baryons is smaller than 0.5% for $z_s > 0.6$ and $100 < l < 1000$. But at $1000 < l < 10000$, the baryons can increase C_l by up to 10 percent depending on z_s. Again, the relative change of C_l increases with the decrease of z_s.

Compared to the previous study of Zhan & Knox (2004) for the effect of hot baryons, our prediction for $\Delta C_l/C_l$ in the non-radiative run is quite different from their finding of a monotonic decline of $\Delta C_l/C_l$ with l at $l > 1000$. We argue that the main reason for this is that they neglected the back reaction of the thermal baryons on the dark matter in their analytical modeling.

To match the accuracy of future lensing surveys, matter power spectrum at scales discussed in this *Letter* must be calibrated to $\sim 1\%$ accuracy (Huterer & Takada 2005). Thus, the baryonic effect is non-negligible for future lensing analysis. Here, we do a simple estimation to demonstrate this point. The statistical errors of lensing

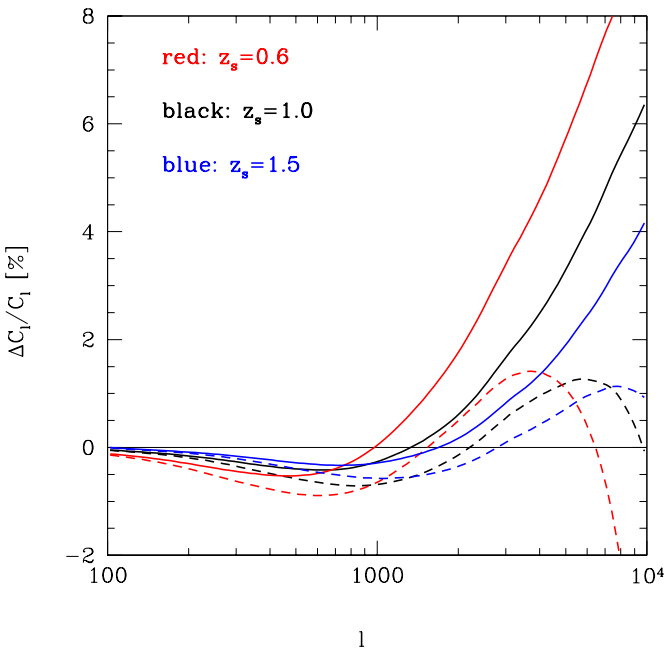

FIG. 3.— The effect of baryons on the shear power spectrum C_l, expressed as relative difference (in percent) to the pure dark matter model. Here the source galaxies are assumed to be at redshifts $z_s = 0.6$, 1.0 and 1.5, respectively. The dashed lines are the predictions from our non-radiative run, while the solid lines give the results for the star formation run.

power spectrum measurements (assuming Gaussianity) are

$$\frac{\Delta C_l}{C_l} = 1\% \left[\frac{l}{1000}\frac{\Delta l}{100}\frac{f_{\rm sky}}{0.1}\right]^{-1/2} \left(1+\frac{\gamma_{\rm rms}^2}{\bar{n}_g C_l}\right), \qquad (2)$$

where n_g is the galaxy number density, with typical value $\lesssim 100/\mathrm{arcmin}^2$, and $\gamma_{\rm rms} \sim 0.2$ is the rms fluctuation caused by the galaxy ellipticities. At $l \lesssim 3000$, the shot noise term is sub-dominant. For future lensing missions with fractional sky coverage $f_{\rm sky} \gtrsim 0.1$, changes in C_l caused by baryons are comparable to, or larger than statistical errors, at $l \gtrsim 1000$. To constrain cosmology using measured C_l's at all accessible scales (l less than several 10^4), the effects due to baryons have to be taken into account. Otherwise the derived constraints can be biased. For example, since $C_l \propto \Omega_m^{\sim 1.2}\sigma_8^2$ (e.g. Van Waerbeke et al. 2001), neglecting this effect can lead to an overestimate of $\Omega_m^{\sim 0.6}\sigma_8$ by several percent. Also, it can cause an overestimate of the initial power index n. To avoid such biases, an accurate modeling of the baryonic effects using hydrodynamical simulations is required.

On the other hand, a precision measurement of the lensing signal at l of about a few thousand could be used to observationally determine the baryonic effects and to constrain the galaxy formation process. This can be done in two steps. One first uses the lensing power spectrum at $l \lesssim 1000$ to constrain Ω_m, $\Omega_{\rm DE}, \sigma_8$, etc. Even though this uses only part of the information in the lensing power spectrum, the cosmological constraints obtained are not significantly degraded (Huterer & White 2005). The derived cosmological model is then used to predict C_l (and its statistical fluctuations) at $l \gtrsim 1000$, assuming no baryonic effects. One can then quantify the deviation of the measured C_l at $l \gtrsim 1000$ from the predicted C_l.

4. CONCLUSIONS

In this *Letter*, we used a controlled set of high resolution N-body and hydrodynamical/N-body simulations to study the influence of baryons on the clustering of cosmic matter. Since the three simulations we used have identical initial condition, simulated power spectra suffer essentially the same sample variance. Since we quantify the baryonic effect as ratios of corresponding power spectra, the result presented in this *Letter* is effectively free of sample variance. In both the non-radiative simulation and the simulation with gas cooling and star formation, the clustering of the gas is suppressed while that of dark matter is boosted at $k > 1\,h\mathrm{Mpc}^{-1}$. The stellar mass is highly biased relative to the dark matter in the pure N-body simulation. Despite a partial counterbalance between the dark matter and the gas, the clustering of the total matter is suppressed by up to 1% at $1 \lesssim k \lesssim 10\,h\mathrm{Mpc}^{-1}$, and is boosted up to 2% in the non-radiative run, and 10% in the star formation run at $k \approx 20\,h\mathrm{Mpc}^{-1}$. Using these power spectrum measurements to study the baryonic effect on the weak lensing shear measurement at $100 < l < 10000$, we found that baryons can change the shear power spectrum by less than 0.5% at $l < 1000$, but by 1% to 10% at $1000 < l < 10000$. Therefore, the influence of baryons on the clustering of cosmic matter will be detected in future weak lensing surveys. Understanding these baryonic effects is not only important for galaxy formation, but also crucial for accurately determining cosmological parameters with cosmic shear, and for constraining the initial fluctuations on small scales.

The simulations were run at Shanghai Supercomputer Center. The work at Shanghai is supported by the grants from NSFC (Nos. 10125314, 10373012, 10533030) and from Shanghai Key Projects in Basic research (No. 04JC14079 and 05XD14019). PJZ is supported by the *One Hundred Talents* project of Chinese academy of science.

REFERENCES

Bell, E. F., McIntosh, D. H., Katz, N., & Weinberg, M. D. 2003, ApJS, 149, 289
Bernardeau, F. 1998, A&A, 338, 375
Dodelson, S., & Zhang, P. 2005, Phys. Rev. D, 72, 083001
Dodelson, S., Shapiro, C. & White, M. 2005, astro-ph/0508296
Fukugita, M., Hogan, C. J., & Peebles, P. J. E. 1998, ApJ, 503, 518
Heymans, C., et al. 2005, astro-ph/0506112
Hou, Y. H., Jing, Y. P., Zhao, D. H., Börner, G. 2005, ApJ, 619, 667
Hu, W. 2002, Phys. Rev. D, 66, 083515
Huterer,D. 2002, Phys. Rev. D, 65, 063001
Huterer, D., & Takada, M. 2005, Astropart.Phys., 23, 369
Huterer, D., & White, M. 2005, Phys. Rev. D, 72, 043002

Ishak, M., Upadhye, A., & Spergel, D. N. 2005, ArXiv Astrophysics e-prints, arXiv:astro-ph/0507184
Jain, B., & Taylor, A. 2003, Physical Review Letters, 91, 141302
Jain, B., Jarvis, M. & Bernstein, G., 2005, astro-ph/0510231
Jarvis, M. & Jain, B., 2004, astro-ph/0412234
Jing, Y. P. 2005, ApJ, 620, 559
Knox, L., Song, Y. -., & Tyson, J. A. 2005, ArXiv Astrophysics e-prints, arXiv:astro-ph/0503644
Limber, D. N. 1954, ApJ, 119, 655
Lin, W.P. et al., in preparation.
Makino, N., Sasaki, S., & Suto, Y. 1998, ApJ, 497, 555
Ménard, B., & Bartelmann, M. 2002, A&A, 386, 784
Rasia, E., Tormen, G., & Moscardini, L. 2004, MNRAS, 351, 237
Schneider, P., van Waerbeke, L., Jain, B., & Kruse, G. 1998, MNRAS, 296, 873
Scranton, R., et al. 2005, ApJ, 633, 589
Springel, V. 2005, MNRAS, 999
Springel, V., & Hernquist, L. 2003, MNRAS, 339, 289
Springel, V., Yoshida, N., & White, S. D. M. 2001, New Astronomy, 6, 79
Takada, M., & Jain, B. 2004, MNRAS, 348, 897
Van Waerbeke, L., et al. 2001, A&A, 374, 757
White, M. 2004, Astroparticle Physics, 22, 211
White, M. 2005, Astroparticle Physics, 23, 349
Zhan, H., & Knox, L. 2004, ApJL, 616, L75
Zhang, P.J. & Pen, U.L., 2006, MNRAS, in press. astro-ph/0504551
Zhang, P.J. & Pen, U.L., 2005, Phys. Rev. Lett., 95, 241302